Geosciences Journal
Vol. 14, No. 2, p. 135 − 153, June 2010
DOI 10.1007/s12303-010-0014-4

Some large values of in-situ stress and related engineering geological problems in China

Yanjun Shang — *Key Laboratory of Engineering Geomechanics, Institute of Geology and Geophysics, Chinese Academy of Sciences, PO Box 9825, Beijing 100029, China*
Hyeong-Dong Park* — *Department of Energy Systems Engineering, Seoul National University, Seoul 151-744, Republic of Korea*
Yongyue Shi, Guangxiang Yuan, Yuanchun Sun — *Key Laboratory of Engineering Geomechanics, Institute of Geology and Geophysics, Chinese Academy of Sciences, PO Box 9825, Beijing 100029, China*

ABSTRACT: In recent years, different methods have been applied to in-situ stress estimation for stability analysis of increasing large-scale tunnels in China. It was found that some extraordinary stress values are mostly associated with, although not a necessity of, engineering geological problems such as collapse, rock burst and squeezing. This paper focuses on finding the relationship among abnormal in-situ stress component values. The exposure in ground surface with unloading and erosion contributes a lot to relatively higher horizontal stress and lateral coefficient values of igneous and metamorphic rocks, while this situation is not the case for sedimentary rocks. Comparing stress data and connecting some abnormal values with typical case examples for better understanding and estimating stress is the main feature of this paper.

Key words: in-situ stress, case examples, engineering geological problems

1. INTRODUCTION

Since Hast (1958) reported that horizontal stress is 1~2 times or even larger than the vertical stress at a number sites in Scandinavia, the observation that horizontal stress dominates at shallow depths, and then it is replaced by vertical stress at larger depths, has often been reported (Brown and Hoek, 1978; Bai and Li, 1982; Wang et al., 1984; Xue et al., 1987). Leeman (1964) published a comprehensive review of the state of development of rock stress determination in 1964. Of 44 papers and reports cited in the review, the two earliest were published in 1954. A set of approaches for the estimation of different kinds of stress was published by Sun (1993). In 2003, Fairhurst presented an historical overview of the need for rock stress information and the nature of rock engineering problems, discussed stress and stress estimation, and gave a review of the stress measurement techniques. Also in this special issue of the International Journal of Rock Mechanics and Mining Sciences, 4 parts as Suggested Methods (SMs) by International Society for Rock Mechanics (ISRM) on rock stress estimation were contained. The 4 parts are together with a suite of supporting papers on various aspects of establishing the rock stress state.

In recent years, one of the most obvious progresses of rock stress is the World Stress Map (WSM), which is the global compilation of information on the present-day stress field of the Earth's crust with 21,750 stress data records in its current WSM database (Heidbach et al., 2008). And some regional or national stress maps, e.g., web site of the Chinese stress map based on 5,335 stress data records mostly in the mainland of China (Xie et al., 2007) (Fig. 1), an review of a decade's hydrofracturing experiences of in-situ stress measurement from 1994 for tunnel construction in Korea based on at least 10 data records (Choi, 2007), and application of hydrofracturing method in Singapore granite (Zhao et al., 2005), were completed.

For the 10 methods used for in-situ stress estimation, the mostly commonly used one is the earthquake focal mechanism (FM), next is borehole breakout (BO), geologic fault-slip (GF), overcoring (OC), and hydraulic fracturing (HF). The seldom used three are borehole slotter (BS), petal centerline fracture (PC) and shear wave splitting (SW), which accounts for less than 0.2% respectively (Fig. 1).

In most cases of rock engineering applications, some unexpected engineering geological problems occurred, where stresses play a key role, they alone are not the critical factor. These problems imply at least two unfavorable aspects. One is that the magnitudes of rock stress values are more important to design and excavation than their orientation, the latter in many areas is already determined qualitatively before measurements in engineering practice. Another reason is that in some complicated engineering geological conditions, both magnitude and orientation vary with time and location. Since a Ms = 7.8 earthquake occurred in Tangshan, North China on July 28, 1976, it has been known that stress for the same region varies with time (Yu et al., 1983). In the Erlangshan Tunnel in western China, the orientation of maximum in-situ stress measured by the HF was NE48.3~50.5° in 1998

*Corresponding author: hpark@snu.ac.kr

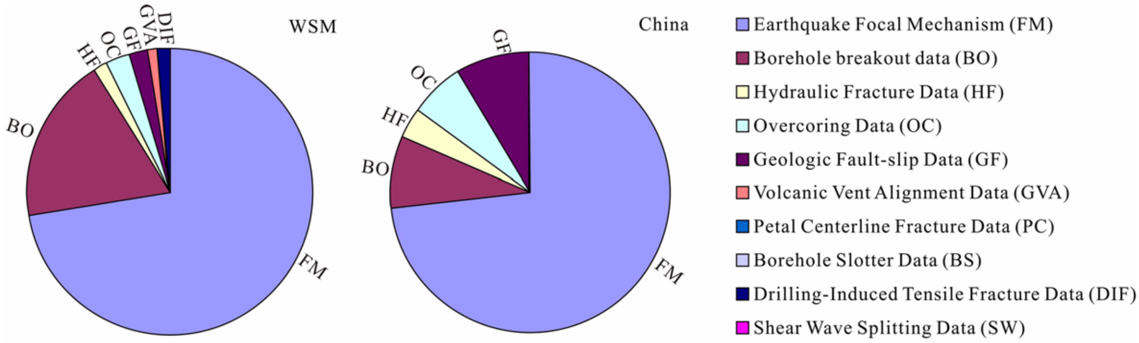

Fig. 1. Proportion of various rock stress data respectively from WSM and China.

(Wang, 1998). However, the orientation by the OC changed to N66.9~85.4W (Xu et al., 2003) when a serious rock burst occurred in the middle part of the tunnel during excavation in 2003. After drilling core discs in the valley banks at the Ertan dam site (Bai and Li, 1982), where the maximum horizontal principal stress (S_H) reaching 66 MPa at a shallow depth of 40 m, it was known that in-situ stress magnitude was obviously and intensively varied with locations. So the state of stress in rocks will remains a topic of major interest in engineering geology and rock mechanics.

In the main land of China, stress data are becoming more and more abundant with the development of various tunnel constructions in hydroelectric schemes, transport lines and mining. For instance, in the end of 2008, the number of highway tunnels was already 5426 nos., and the length of tunnels was 3186.4 km. Before 2010, the length of highway reached 3.8282×10^6 km, of expressway reached 6.5×10^4 km (Fig. 2). Obviously, the total length of highway tunnels will be over 3200 km.

In most cases unexpected engineering geological problems such as collapse, squeezing or rock burst occurred due to high rock stress in tunneling. The problems are closely associated with dubious high stress often without stress measurements or with unfeasibility for measurement in current methods. Therefore, it is necessary to check whether the abnormal values are associated with some critical engineering geological problems. Usually, measurements in several locations are necessary to extrapolate the results with confidence to other situations. The purpose of this paper is to present the updated overview of ranges of high values of stress and coefficients, and to explain some engineering geological problems in terms of large stress values by comparing the three components of in-situ stresses.

2. METHODS AND TECHNIQUES

2.1. In-situ Stress Tests

There are two kinds of fundamental methods for measuring in-situ stress (Fig. 3). One is a quantitative measurement, the other is a qualitative estimation. The commonly adopted are OC (Sjoberg et al., 2003) and HF (Haimson et al., 2003) (Fig. 1). So methods and techniques are developed and modified accordingly. The HF, OC, GF and FM are undertaken from shallow to large depth, as 1 km, 1~5 km, upper part of the crust, and middle to upper part of the crust, respectively, which provide data records for this paper. The OC and HF methods providing results are analyzed in this

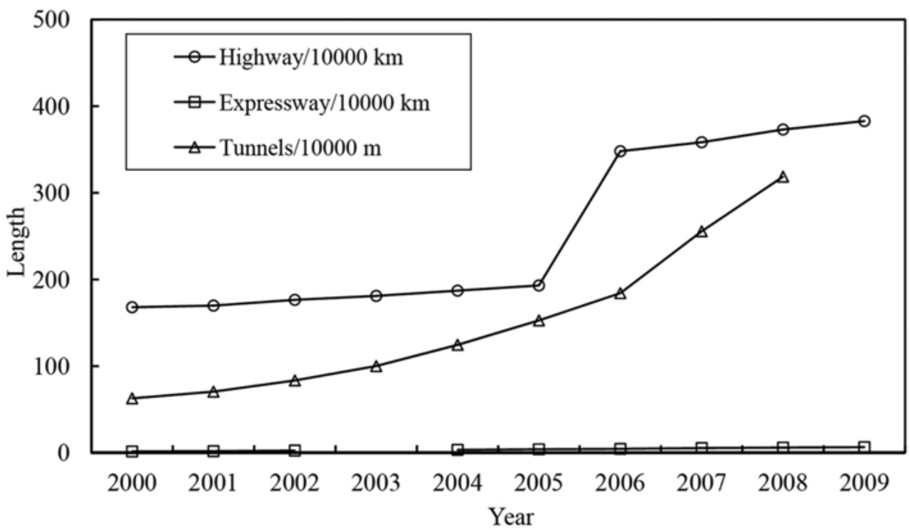

Fig. 2. Increasing length of highways and tunnels in China in recent years.

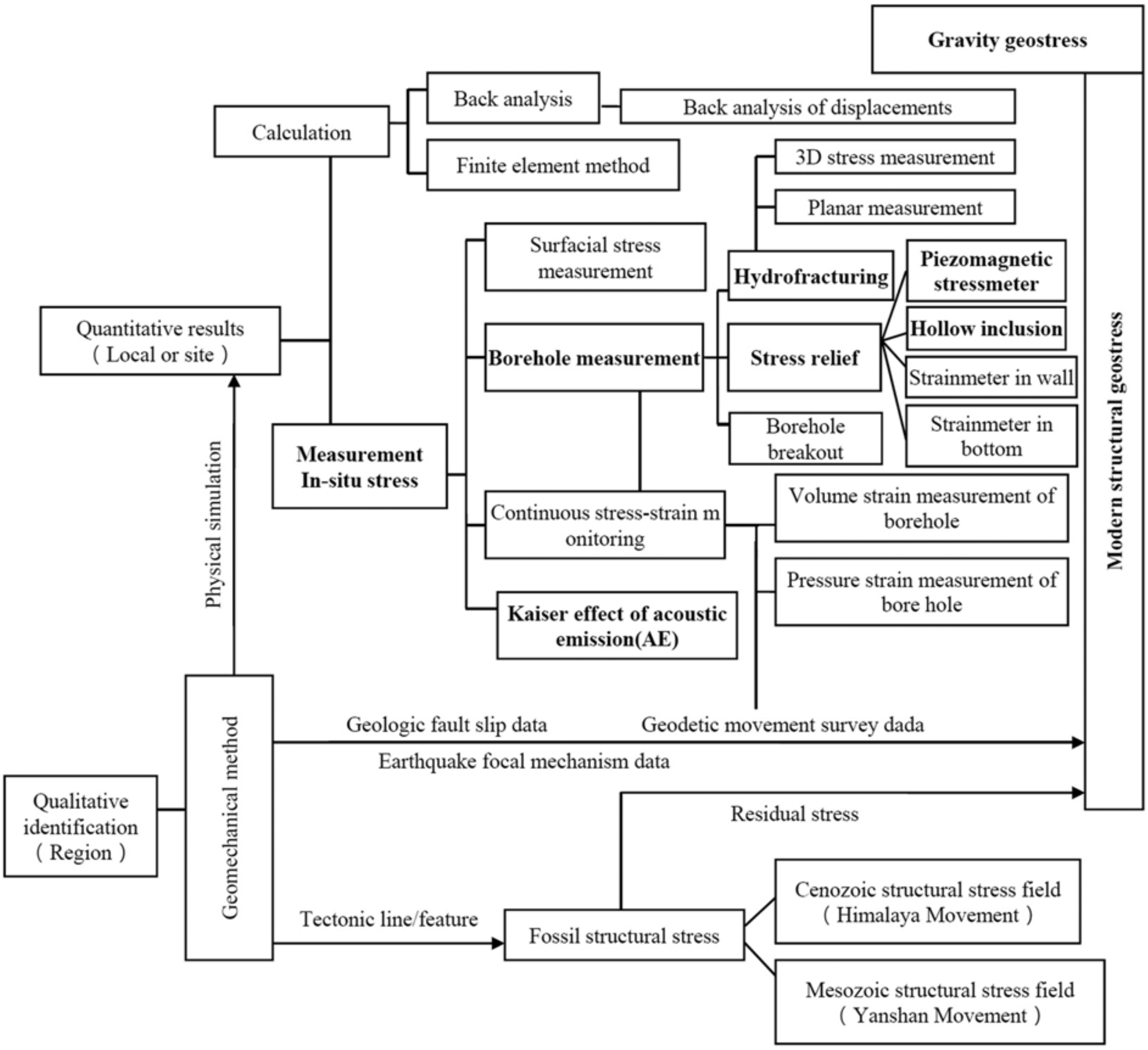

Fig. 3. Methods and techniques for identification and test of in-situ stress.

paper. In China, HF reaches 1,104 m depth in the Wanfu Coal mine (Cai et al., 2006). In-situ stress is calculated from HF produced under high pressure in petroleum exploration to depths of over 2000 m (Qiao et al., 2001). In tunnels during excavation, the OC or stress relief technique is widely accepted in sub-horizontal and vertical boreholes to test the stress status of surrounding rocks outside the excavation damaged zone (EDZ) together with tunnelling. The HF is widely adopted in field investigation in boreholes. Some specimens were sampled on site and taken to the laboratory for acoustic emission tests (AE) based on Kaiser effect (Boyce, 1981). These techniques and methods have their own advantages and disadvantages (Table 1). Generally, five quality ranks (A~E) are assigned to qualify the stress data records from different methods and techniques (Heidbach et al., 2008). A quality means that the orientation of the S_H is accurate to within ±15°, B quality to within ±20°, C quality to within ±25°, and D quality to within ±40°. The WSM and analysis on stress patterns and interpretation are generally based on those higher qualified records (A~C), which accounts for 79% of the total 21750 WSM release in total in 2008 (Heidbach et al., 2008). The data used in this paper is cited from various referential papers and reports for engineering use with orientation and quantity, not from officially reported in WSM. Thus these data are generally highly ranked above C.

2.2. Compilation of Stress Data

In this paper, 1142 data records of in-situ stress selected from published data with lithology from 13 regions and countries including Australia, Canada, China, Scandinavia, South Africa, USA, Japan, etc. were used. The three types of rocks, namely igneous (Ig), sedimentary (Sed) and meta-

Table 1. Comparison of methods and techniques for identification of in-situ stress

		Hydrofracturing method (HF)	Overcoring (Stress relief) method (OC)	Acoustic emission from Kaiser effect (AE)	Back analysis method (BA)
Application condition	Location	Bore holes from ground surface or in tunnels	Shallow boreholes in tunnels	Laboratory test on sampled specimen	In laboratory via computer and software with monitored data (displacement, force)
	Depth/m	1104~ (Cai et al., 2006)	1400~ (Liu et al., 2004; Liu and Xiao, 2005)	No limit (Boyce, 1981)	No limit (Yang et al., 2001)
Advantage		(1) Principle easy understand (2) Quick resolution (3) Tests at different depth of same locations (4) Suggested method by ISRM, common use in competent rocks and in field investigation	(1) Easy installation (2) Near concerned site (3) High efficiency with 3D (4) Higher suitability to poor geological conditions (5) Suggested method by ISRM, wide use in mining sites and in excavation stages	(1) Easy and economical use (2) Principle easy understand (3) Can do in large amounts of samples	(1) Easy, quick and economical (2) Closely connected with excavation and supporting design
Disadvantage		(1) Vertical boreholes with effects of 2-D (2) The vertical stress is calculated (3) Affects from fractures and joints in monitored section (4) Depth limits (5) Lower grade of automation	(1) Different orientations of boreholes (2) Complicated coordinate system transform (3) Difficult to test before excavation (4) Calibration of temperatures.	(1) Effects from fossil stress in geological history (2) Effects of rock strength	(1) only after obtained monitored data (2) Effects from disturbed zone (3) Effects from model adopted

Table 2. Numbers of data with different rock types from 13 regions and countries

Region/Country	Igneous rocks	Sedimentary rocks	Metamorphic rocks	Sum
Australia	8	16	31	55
British Island	14	8		22
Canada	14	12	29	55
China	417	302	128	847
Germany	3	3		6
Iceland	2			2
Japan	11	7	2	20
Portugal	1			1
Russia	8			8
Scandinavia	20	5	12	37
Singapore	7			7
South Africa	1	3	15	19
United States	19	40	4	63
Total	525	396	221	1142

morphic (Met), are classified and compared (Table 2). There are 525, 396 and 221 records of Ig, Sed and Met rocks, resepectively. In the legends, the three are marked as *Ig* in red, *Sed* in blue, and *Met* in green colors. Among them the data from China is almost completely selected with respect to HF and OC methods commonly adopted in rock engineering (Yu et al., 1983; Liu et al., 1992; Li et al., 1993; Cai et al., 1997; 2000; Jin et al., 2001; Wu et al., 2004; Zhou et al., 2005; Chen et al., 2006; Zhou et al., 2006; Xiao, 2007). Other national or regional data are mainly from Brown and Hoek (1978), Zhu and Tao (1994). These data were primarily checked and applied in engineering design and construction to pass practical examinations. If some measured points were too close to a working face or susceptible to free face with intensive unloading, and seemed to be unreasonable with, for example, negative (extensive) stress values, then these records were not included in the analysis.

The three components, maximum and minimum horizontal stresses, and vertical stress, are marked as S_H, S_h, and σ_v, respectively. They are drawn from coordinate system transformation, and calculation of space stress tensors measured in sites. In most cases of OC and AE methods, the three components σ_1, σ_2 and σ_3 are obtained with trends and plunges in 3D. The σ_v is also introduced for presentation of the vertical stress with largest plunge values. In the case of the HF, the vertical stress is calculated as the overburden load (gravity) S_v. In some cases of OC in 2D, the vertical stress is also calculated as (Brown and Hoek, 1978):

$$S_v = \gamma H = 0.027H \quad (1)$$

where γ is the average unit weight of the overburden (taken as 0.027 MPa/m in this study), H is depth (m). For the Sed rocks such as mudstone and coals, the γ is approximated to be 0.025 MPa/m.

In previous studies, the coefficient of mean values of horizontal stress ($\sigma_{h.av}$) and vertical stress was denoted by k (Brown and Hoek, 1978).

$$k = \sigma_{h.av} / \sigma_v, \quad (2)$$

$$\sigma_{h.av} = (S_H + S_h) / 2. \quad (3)$$

For underground engineering design, the engineers are more concerned with the S_H than with the σ_v. The ratio (λ) of S_H to σ_v is expressed as follows (Bieniawski, 1984).

$$\lambda = S_H / \sigma_v. \quad (4)$$

As by-products of HF in boreholes, the tensile strength (T_{hf}) and shear stress (τ), representing the rock status in the measured section, can be obtained from data-log parameters. They include breakdown pressure (P_b), the fracture reopening pressure (P_r), the shut-in pressure (P_s) and pore pressure (P_0).

$$T_{hf} = P_b - P_r, \quad (5)$$

$$\tau = (S_H - S_h) / 2. \quad (6)$$

In Equation (6), the maximum shear stress τ acts on vertical plane whose azimuth is 45° from the orthorhombic axis of S_H and S_h. From the data log they two can be calculated as (Haimson and Cornet, 2003)

$$S_h = P_s, \quad (7)$$

$$S_H = 3P_s - P_r - P_0. \quad (8)$$

From Equation (7), it is known that the P_s is the pressure needed to equilibrate the fracture-normal stress S_h. From the bilinear curve of fracture opening and closing phase, the point of intersection of the curve is taken as the P_s (Rutqvist and Stephansson, 1996). In practice the P_s is obtained as one average of the consistent multiple cycles in HF.

The P_0 in most cases is not measured but assumed to be as hydrostatic as buried in depth under water table. Utmost care must be taken in selection of measured section to prevent original fissures or joints for obtaining high quality HF curves. So the drill core observation and core logging quality are important for the test parts selection in bore holes.

In the Chinese standards (IYRWR, 1995), the evaluation of rock mass ranks is determined by the ratio (R) of uniaxial compression strength (σ_c) to maximum principal stress (σ_{max}) perpendicular to tunnel strike.

$$R = \sigma_c / \sigma_{max}. \quad (9)$$

If $4 < R < 7$, then it is high stress. If $R < 4$, then it is very high stress. These limitary values are often used for identification of rock burst.

In many cases, at least two methods have been adopted to process in-situ stress data due to complicated geological conditions or the importance of the geo-engineering projects. For the data group in one location, the maximum or minimum values were selected, and the mean values were equal to their sums divided by the number of records. But this is changed in considering the trend. They were calculated according to positive or negative values, clockwise from the north direction. And in many cases, the large variation in shallow depth was overlooked and was normally replaced by relatively stable values measured at a deeper part of the same borehole.

During processing of the data, some abnormal values were related to the interpretation of the engineering geological problems, especially for those in China, to clarify some engineering geological problems in tunneling, which occurred more and more in western China. More importantly, these stress values could provide some clues for solutions to the existing problems as for consolidation or modification of tunnel shapes.

2.3. Diagrammatic Presentation of Stress Data

In processing in-situ stress data, the stereographic projection method with the upper hemisphere and equal angles are used. The orientation of S_H is in the form of a rosette plot, with five max planes at the outer circle and the trend of face normal = 0.9. The vector is in the form of a pole plot, with square marks for σ_1, x-crosses for σ_2, and triangles (up) for σ_3. In the cases of S_H, S_h and S_v, the marks are also squares, x-crosses and triangles.

3. RESULTS

3.1. Comparison of the Three Components

From the 1142 records of in-situ stress data from various countries as listed in Table 2, it is known that the three components differ with lithology and depth (Fig. 4). Some extraordinary values are marked with numbers. The numbers in parenthesis are concordant with those cases listed in Table 3 and other numbers are concordant with those in Table 4. Most of the data are from depths less than 1,000 m, within which the S_H of Ig has the largest variation and values. The Met obviously has scattered values in depths between 1,000 and 2,000 m. The scattered spots also indicate that the Ig has the largest gradients of S_H with depth, while the Sed has the smallest but behave more regularly (Engelder, 1993).

From Figure 4 it is known that within depths of 1,000 m, the largest S_H values are 90 and 78 MPa in the granite of Scandinavia (Hast, 1973) and in ijolite of Kolskiy Pov, Russia (Pine et al., 1983), respectively.

From Table 3, it can be seen that most of the largest values of S_H are from the Ig and Met in Scandinavia, China, Canada, and Russia. In the United States, at a depth of 5,108 m, it is known that S_H is as large as 135 MPa. At shallow depth less than 100 m, the largest value is 65.9 MPa measured using the OC technique in boreholes in syenite at gorge banks at Ertan, southwest China (No 29–1 as listed in Table 4).

From Figure 5, it is generally seen that the ratio of S_H to

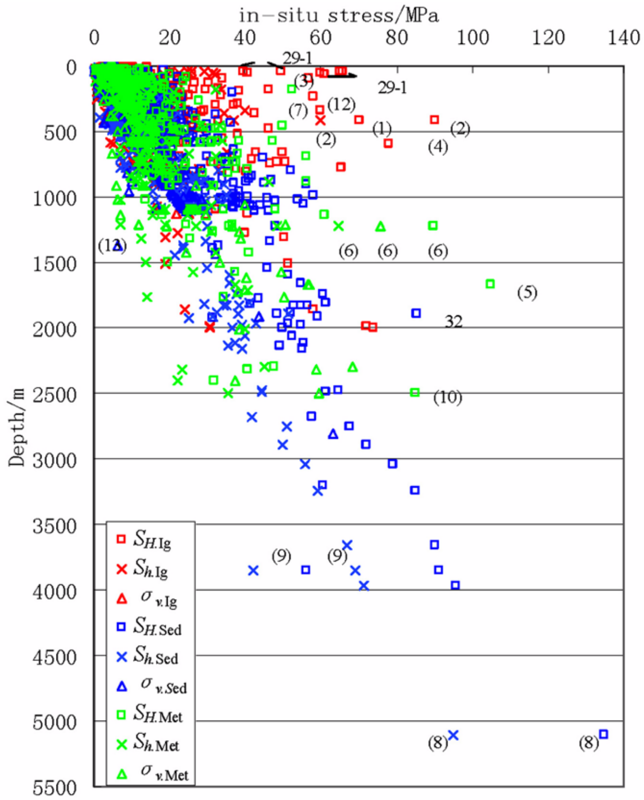

Fig. 4. Variation of in-situ stress components with lithology in depth.

S_v is the largest; the λ is the second, and k is the smallest value. Also it was found that within depths of 800 m, all stress values for Ig are obviously larger, while for the Sed the smallest values of coefficients. If the data are compared to the two boundary lines, i.e., $k = 1500 / H + 0.5$ at the right and $k = 100 / H + 0.3$ at the left, as suggested by Brown and Hoek (1978), it shows that at shallow depth (<300 m), some smaller k values are out of the left boundary line, while in depth of 300 to 1,000 m, some spots representing the Ig and Met are out of the right boundary line. Usually, in depth over 1,300 m, the k is mostly no bigger than 2.0. The biggest one as $\lambda = 5.29$ at spot (13) is from one oil field in North China, due to a very small value of S_v (not measured as σ_v) from smaller unit weight values (shale and siltstone) (Chen et al., 1982). When at depth below 2,000 m, it is nearly 1.0 (the dot-dashed line). The one abnormal value as $\lambda = 1.26$ is from South Africa with quartzite at a depth of 2,500 m with $S_H = 85.08$ MPa (Gay, 1975).

Figure 6 presents the large variations of vertical stress σ_v when compared to the overburden load S_v. It reminds us that the results from HF in 2D and from OC in 3D are generally different in some steep valley banks. The relation of the two values varies with depth. In depths less than 300 m, usually $\sigma_v > S_v$; while in depths between 300 and 1,000 m usually $\sigma_v < S_v$. In depths between 1,000 and 1,800 m, the trend is mixed and the most obvious difference is at spot (6) in quartzite in Canada. At depths more than 1,800 m, $\sigma_v < S_v$. At depths over 800 m for the Sed, the σ_v is always smaller.

As another form of presentation, Figure 7 reveals directly the relationship of σ_v versus S_v. It shows that in a range of less than 20 MPa, the two values are very scattered, generally $\sigma_v > S_v$. In the range of 20 to 30 MPa, the sequence of the two values are reversed. In the range of 30 to 50 MPa, the trend is mixed, but when the stress is larger than 50 MPa, $\sigma_v < S_v$. Thus, it can be inferred that in a depth less

Table 3. Some sites with extraordinary in-situ stress values

No.	Country	Region	Lithology	Depth (H/m)	Maximum horizontal stress S_H/MPa	Minimum horizontal stress S_h/MPa	Vertical stress σ_v/MPa	Reference
(1)	Finland	Scandinavia	granite	410	70	37		Hast, 1973
(2)	Finland	Scandinavia	granite	410	90	60		
(3)	Russia	Kolskiy Pov	ijolite	100	57	23	23	Pine et al., 1983
(4)	Russia	Kolskiy Pov	ijolite	600	78	15	18	
(5)	Canada		quartzite	1669	105.04	37.49	56.74	Linder and Haipern, 1978
(6)	Canada		quartzite	1220	89.64	48.27	75.85	
(7)	Canada		quartz schist	177	52.59	11.77		
(8)	USA	Michigan	shale	5108	135	95		
(9)	USA	Mecigen	shale	3850	56	42		
(10)	South Africa		quartzite	2400	31.78	22.11	37.41	Gay, 1975
(11)	South Africa		quartzite	2500	85.08	35.58	59.34	
(12)	China	Liaoning	basalt	230	57.93	7.18	14.2	Liang and Pan, 1989
(13)	China	North China oil field	sandstone	1374	32.8	23.58	6.2	Chen et al., 1982
(14)	USA	Nevada	fragments	434	4	3.55	2.41	Imrie and Jory, 1968
(15)	Australia		gneiss	1022	13.5	7.16	6.21	Wototniki and Denham, 1976
(16)	Australia		quartzite	1140	18	15.6	6.9	

Table 4. List of some case examples with in-situ stress results in China

No.	Project name	Location	Strike (°)	Lithology	Depth (H/m)	Length/ width (m)	S_H strike (°)[a]	Inclin-ation of axis with S_H(°)	S_H/MPa[a]	S_h/MPa[a]	Engineering geological problems	Test section	Test method /technique	Reference
1	Huanggou pumped storage power station	Mudanjiang, Heilongjiang	N49 W	granite	350	130/50	80–319 /282(5)		7.5–11 /9.24(5)	3.1–7.3 /5.58(5)		5 records from 11 measured sections at 4 points	Hollow inclusion of stress relaxation	Wu et al., 2002
2	Hongtoushan copper mine	Fushun, Liaoning	EW	gneiss	317–1217		NNW–NW	50	11.5–36.6 /22.87(6)	5.9–18.8 /11.77(6)	Failure, caving, rock burst	8 measured points in 5 levels	Hollow inclusion of stress relaxation	Wu and Liao, 2000
3	Pushihe pumped storage power station	Kuandian, Liaoning		granite	200		281		3.4–12.7 /6.72(10)	1.3–5.9 /3.05(10)		5 measured points in 2 adits with 10 records	Hollow inclusion of stress relaxation	Wu et al., 2006
4	Jinzhou cavern	Jinzhou, Liaoning		granite	28.1–133.7		73		3.92–12.64 /9.26(38)	3–9.02 /5.69(38)		38 measured sections in 5 boreholes with 17 mould sections	Hydraulic fracturing	Hou et al., 2006
5	Shanshandao gold mine	Laizhou, Shandong	40	granite	105–150		40~49		9.32–11.28 /10.30(2)	4.61–7.65 /6.13(2)	S_H:S_v:S_h = 1:0.9:0.65	2 measured points in 2 levels	Hollow inclusion of stress relaxation, AE	Yao et al., 1995
6	Wanfu coal mine	Juye, Shandong		sand-stone, coal	790.5–1104.4		32.6–110.6/ 59.77(21)		26.35–58.01 /37.86(37)	20.34–35.2 /25.18(37)		37 measured sections in 7 bore holes	Hydraulic fracturing	Cai et al., 2006
7	Datun coal mine	Xuzhou, Jiangsu		coal	387–819		NNE–NNW		8.85–23.04 /13.98(7)	5.38–16 /9.94(7)		7 measured points in 6 bore holes	Hollow inclusion of stress relaxation	Zhou et al., 2007
8	Anqing copper mine	Huaining, Anhui		diorite	280–580		47–267 /240(6)		11.9–24.4 /17.31(10)	4.4–13.1 /7.91(10)		10 measured points in 3 levels	Hollow inclusion of stress relaxation	Dong et al., 2001
9	South Fujian Tunnel	Highway, south Fujian		granite	124–421				6–13.9 /9.63(10)	4.4–9.3 /6.86(10)		10 measured sections in 1 borehole	Hydraulic fracturing	Yin et al., 2001
10−1	Guangdong pumped power station	Conghua, Guangdong		granite	150–497.5		N50~60W		2.59–10.68 /7.65(15)	0.63–9.01 /5.59(15)		21 measured points in 15 measured sections in 4 boreholes	3D strainmeter in bore-holes	Liu et al.,1990
10−2	Guangdong pumped power station I stage	Conghua, Guangdong		granite	27.04 –203.8		276–347 /320(7)		4.28–18.5 /10.92(22)	4.03–10.42 /6.94(22)		22measured sections in 3 boreholes with 9 sections of moulds	Hydraulic fracturing	Sun et al., 1991
10−3	Guangdong pumped power station II stage	Conghua, Guangdong		granite	92.17–505.21		280–323 /305(6)		6.72–15.64 /12.52(19)	4.92–9.3 /7.67(19)		19 measured sections in 2 boreholes with 11 sections of moulds	Hydraulic fracturing	Guo et al., 2002
11	Daya Bay tunnel	Shenzhen, Guangdong		granite	18.48–204.23		271–327 /296(7)		4.55–13.05 /8.03(17)	3.38–7.63 /5.33(17)		17 measured sections in 2 bore holes with 7 sections of mould	Hydraulic fracturing	Tan et al., 2006
12	Damao tunnel	Highway of east Hainan	302	granite	14–18	1000	282.5	19.5	3.1–3.3 /3.2(2)	1.7–2 /1.85(2)		2 bore holes	Piezomagnetic method of stress relaxation	Wu and Liao, 2000
13	Xiaolangdi hydroelectric power station	Jiyuan, Henan	135	sandstone	80–135		58–95 /76.5(2)	58.5	1.49–3.56 /2.53(2)	0.96–2.35 /1.66(2)		1 and 2# adits at left bank	AE	Feng, 1996

Table 4. (continued)

No.	Project name	Location	Strike (°)	Lithology	Depth (H/m)	Length/ width (m)	S_H strike (°)[a]	Inclin-ation of axis with S_H(°)	S_H/MPa[a]	S_h/MPa[a]	Engineering geological problems	Test section	Test method /tech-nique	Reference
14	Pingdingshan caol mine	Pingdingshan, Henan	285–305	sandstone	555–633		122.6–216.8 /164(3)	3959	20.82–33.02 /26.48(3)	12.62–17.85/ 14.73(3)		3 measured points	Hollow inclusion method of stress relax-ation technique	Gou and Zhang , 2002
15–1	Three Gorges reservior	Zigui, Hubei		sandstone	393.25–498		16–66 /42.6(4)		9.91–22.37 /16.69(7)	5–13.99 /10.63(7)		1 bore hole	Hydraulic fracturing	Yuan et al., 1996
15–2	Three gorges dam site	Maoping, Hubei		granite	154–790		280–331/ 298.6(5)		12.05–22.5 /16.35(16)	6.8–14.64 /10.28(16)		1 bore hole	Hydraulic fracturing	Li et al.,1993
15–3	Three Gorges shiplock	Shandouping, Hubei	107	granite	40.8–303.3	1000	55	52	4.9415.36 /8.76(14)	0.977.6 /4.17(14)		13 measured sections in 2 boreholes, 9 mea-sured points in 2 adits	Stress relaxation	Liu et al.,1992
16–1	Baozhen tunnel of Yiwan Rail-way	Changyang, Hubei	90	shale, silt-stone limestone	150.31–479.58	11608	113–123 /118(3)	28	7.1–21.7 /13.69(16)	5.1–13.3 /8.94(16)	Large defor-mation	1 bore hole	Hydraulic fracturing	Xiao et al., 2005
16–2	Baziling tunnel of Yiwan Railway	Changyang, Hubei	309	limestone	59.2–545.8	5867	68–81 /75.7(3)	53.3	1.48–14.95 /9.64(12)	0.99–8.33 /5.33(12)	Karst and rock burst	1 bore hole	Hydraulic fracturing	Xiao et al., 2005
16–3	Yeshanguan tun-nel of Yiwan Railway	Badong, Hubei	279	limestone mudstone	156–458.15	13846	79–91 / 84.3(3)	14.7	8.32–18.88 /13.78(10)	5.06–10.68 /7.95(10)	Large defor-mation	1 bore hole	Hydraulic fracturing	Xiao et al.,2005
17	Xuefengshan tun-nel	Shaoyang, Hunan	290	sandy slate	70.07–778.41	7000	274–303 /290(8)	0	2.16–24.51 /14.56(28)	2–16.45 /9.8(28)		28 measured sections in 3 boreholes with 8 sections of moulds	Hydraulic fracturing	Zhang et al., 2005
18	Yellow river diversion tunnel	Taiyuan, Shanxi	NW	limestone	85.5–303.12		346–350/ 348.5(4)	~60	10.1–20.2 /14.97(15)	4.5–8.8 /6.77(15)		15 measured sections in 2 boreholes	Hydraulic fracturing, AE	Wang et al., 1996
19	Qinling tunnel	Lantian, Sanxi		gneiss	2–		32–83.7/ 60.8(11)		10.82–19.5 /15.16(11)	0.8–12.44 /7.72(11)	Rock burst	11 nos. samples	AE	Chen et al., 1982
20	Bijiashan tunnel	Highway Lk122+180, Chongqing	129	sandstone	369		166	37	5.59	1.90		27 nos. samples	AE	Kang et al.,2005
21	Yongchuan coal mine	Yongchuan, Chongqing		sandy mudstone siltstone	522.25–676.18		36.8–35.4/ 36.1(2)		15.49–17.43 /16.46(2)	7.88–9.19 /8.54(2)		2 measured points	Hollow inclusion method of stress relax-ation	Wei et al., 2007
22	Baijiao coal mine	Gongxian, Chongqing	SE–NW	coal	560–580	7000	273–276/ 274.5(2)	~50	29.3–30.2 /29.75(2)	17.6–18.1 /17.85(2)		2 measured points	Stress relaxation in drilled holes	Su et al., 1994
23	Lubuge hydro-electric power station	Luoping, Yun-nan		dolomite	40–322		290		3.96–17.3 /12.15(6)	0.06–5.21 /3.77(6)		6 measured points	Stress relaxation	Xue et al.,1987
24–1	Jinchuan nickel mine <500 m	Jinchang, Gansu	310	ultra-basic rocks	20–480		318–32 /1(6)	51	2.4–50 /23.01(8)	2.3–33.4 /14.11(8)		10 measured points	Hollow inclusion strainmeter	Liao and Shi, 1983

Table 4. (continued)

No.	Project name	Location	Strike (º)	Lithology	Depth (*H/m*)	Length/ width (m)	S_H strike (º)[a]	Inclin-ation of axis with S_H(º)	S_H/MPa[a]	S_h/MPa[a]	Engineering geological problems	Test section	Test method /tech-nique	Reference
24–2	Jinchuan No.2 mine >500 m	Jinchang, Gansu	310	Ultra-basic rocks	580–790		340–36.6/ 15(10)	65	24.88–40.55 /33.15(10)	9.44–17.66 /13.03(10)		8 measured points	Hollow inclusion strainmeter	Cai et al., 1999
25	Wuqiaoling tun-nel	Tianzhu, Gansu	343	Sandstone phyllite	514–866.53	20050	10–24 /19.5(4)	36.5	15.57–22.32 /19.48(6)	7.56–12.32 /10.46(6)	Large defor-mation	Working face of 5\6\7# inlcine shafts, vertical bore holes at 8 # incline shaft	Hydro-fracturing mea-surement in 3D and plane	Guo et al., 2006
26	Laxiwa hydro-electric power station	Guide, Qing-hai		granite	157–282		303–58 /2.6(5)		17.6–22.87 /20.79(5)	13.29–14.9 /13.83(5)		5 records		Xue et al., 1987
27	West line for water transfer	Ganz, Aba, Sichuan	NE	Sandy slate	24.9–150		12.7–70.1 /44.49(7)		1.06–12.05 /6.24(13)	0.75–7.5 /4.21(13)		7 bore holes	Hydraulic fracturing	Peng et al., 2006
28–1	Erlangshan tun-nel 98	Ya'an, Sichuan	255	Sandstone limestone	79.72–621.52	4176	45.3–50.5/ 48.4(3)	26.6	5.19–36.28 /15.55(33)	4–20.57 /10.14(33)	Rock burst	3 bore holes CZK8~10	Hydraulic fracturing	Wang, 1998
28–2	Erlangshan tun-nel 03	Ya'an, Sichuan	255	Sandstone limestone	760	4176	275–293/ 284.8(8)	29.8	7.8–35.3 /19.72(8)	3.2–8.1 /5.03(8)	Rock burst	2 groups stress relax-ation, 6 groups AE	Stress relaxation, AE	Xu et al., 2003
29–1	Ertan hydroelec-tric power station	Dukou, Sichuan		syenite	17.6–59.4		20		1.8–65.9 /38.25(11)	0.5–32 /18.49(11)	Rock burst	11 measured points in 2 boreholes	Piezomagnetic method of stress relax-ation	Bai and Li, 1982
29–2	Ertan hydroelec-tric power station	Dukou, Sichuan		Syenite basalt	58–345		353–40 /20.4(9)		9.6–38.4 /25.83(9)	4.3–22 /13.18(9)	Rock burst	9 measured points	Stress relaxation	Xue et al., 1987
30	Ahai hydroelec-tric power station	Yulong, Yun-nan	120	Sedimen-tary rocks	92–114.2		305–316 /310(3)	10	3.4–5.1 /4.3(6)	2.5–3.7 /3.13(6)		6 measured sections in 1 borehole with 3 mould sections	Hydraulic fracturing	Zhou et al., 2007
31	Songshuyuan tunnel	Dali, Yunnan	305	limestone	103.4–224		65.5–75.1 /70.3(2)	54.7	4.32–14.68 /10.72(8)	4.1–9.2 /7.46(8)	Rock burst	8 measured sections in 1 borehole, with 2 mould sections	Hydraulic fracturing	Li et al., 2005
32	Baka oil field	Tuha basin, Xinjiang		sandstone	1744.2–2067.45		325		43.7–85.4 /55.71(13)	32.4–51.2 /38.59(13)	Fissures	13 measured sections in 11 oil wells	Estimation from crushing curves	Qiao et al., 2001
33	Tianshan tunnel	North Tians-han, Xinjiang	43	Conglomer-ate, dacitic porphyry	60.67–385	13610	315–25 /350(19)	53	8.62–20.5 /14.64(31)	6.23–14.1 /10.23(31)	Rock burst	31 measured points in 3 boreholes with 19 mould sections	Hydraulic fracturing	Ma et al., 2005
34	Xiabandi hydro-electric power station	Kashi, Xin-jiang	0	Gneiss	27–159.92		206–303.2 /66.93(9)	66.93	4–9.8 /8.02(9)	3–6.35 /4.9(9)		19 measured points in 5 boreholes, 14 measured points in 2 boreholes	Hollow inclusion strainmeter Hydraulic fracturing	Liu et al., 2004; Liu and Xiao,2005
35	Wudaoliang	Wudaoliang, Qianghai	20	diorite			26	6.8	3.2	0.53		1 measured point	Piezomagnetic method of stress relaxation	Wu et al., 2005

Table 4. (continued)

No.	Project name	Location	Strike (°)	lithology	Depth (*H/m*)	Length/ width (m)	S_H strike (°)[a]	Inclin-ation of axis with S_H(°)	S_H/MPa[a]	S_h/MPa[a]	Engineering geological problems	Test section	Test method /technique	Reference
36	Fenghuoshan tun-nel	Fenghuoshan, Qinghai	20	mudstone siltstone	12–16	1334	61–86 /77(3)	57	3.6–5.5 /4.57(3)	1–2.9 /2.23(3)		3 measured points	Piezomagnetic method of stress relaxation	Wu et al., 2005
37	Yanshiping	Yanshiping, Qinghai		fine sandstone	13.5		47		5.6	4.4		1 measured point	Piezomagnetic method of stress relaxation	Wu et al., 2005
38	Anduo	Tibet		granite	14		314		8.1	4.8	Closed to suture zone	1 measured point	Piezomagnetic method of stress relaxation	Wu et al., 2005
39	Yangbajing tunnel	Yangbajing, Tibet		granite	11–13		45–81 /60.25(4)		3.3–10. 4 /6.5(4)	2.5–8.4 /4.58(4)		4 measured points	Piezomagnetic method of stress relaxation	Zhang et al., 2007
40	Lhasa	Tibet		granite	18		322		4	2.6		1 measured point	Piezomagnetic method of stress relaxation	Zhang et al., 2007
41	Qushui	Qushui, Tibet		granite	12		343		2.3	2		1 measured point	Piezomagnetic method of stress relaxation	Zhang et al., 2007
42	Kangma	Kangma, Tibet		granite	13		311		5.2	4.4		1 measured point	Piezomagnetic method of stress relaxation	Zhang et al., 2007

[a]Min–Max/mean (number)

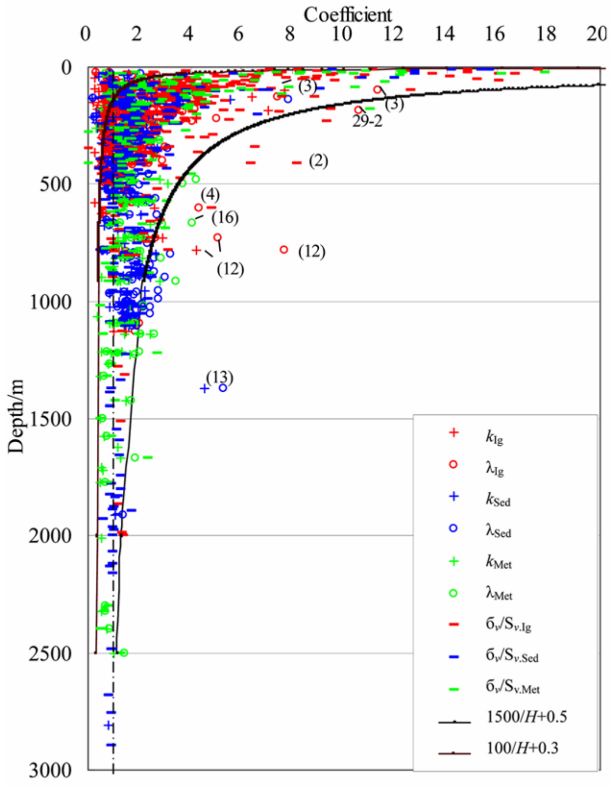

Fig. 5. Coefficient of components of in-situ stress versus depth.

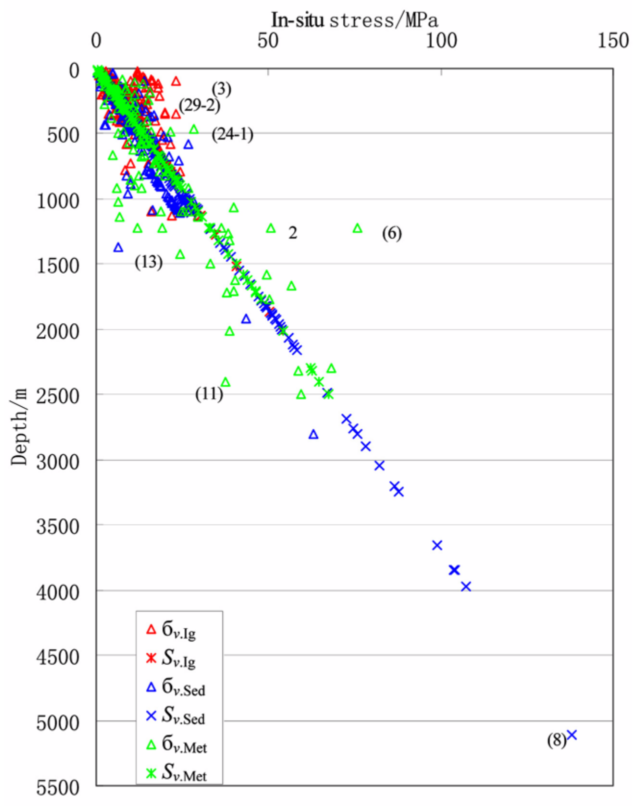

Fig. 6. Comparison of calculated S_v and measured σ_v values of (nearly) vertical component of in-situ stress.

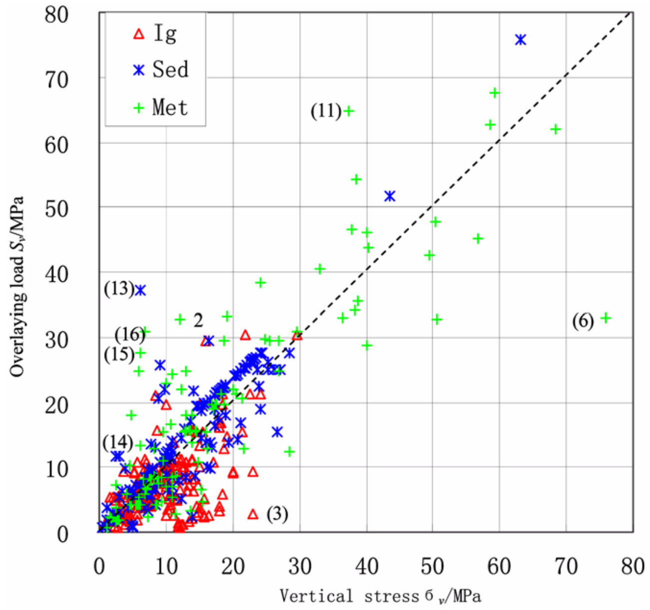

Fig. 7. Relation of σ_v with S_v.

than 300 m, the σ_v is bigger than the S_v due to the effects of lateral stress. When larger than that depth, S_v becomes the bigger one at a depth of 1,000 to 1,800 m where the trend is uncertain. Therefore, in shallow depths, the σ_v cannot be overlooked and can replace the S_v, while in larger depths, the S_v is bigger in some cases.

3.2. In-situ Stress Trends and Plunges

As in most cases, the three components are presented as trends and plunges. For the 220 data records in OC and AE in China, the plunge of σ_1 is in the range of 0 to 30°, while that of the σ_v is mostly in a range of 45 to 85° (Fig. 8) and 45° is an important limit between the plunges of σ_1 and σ_v.

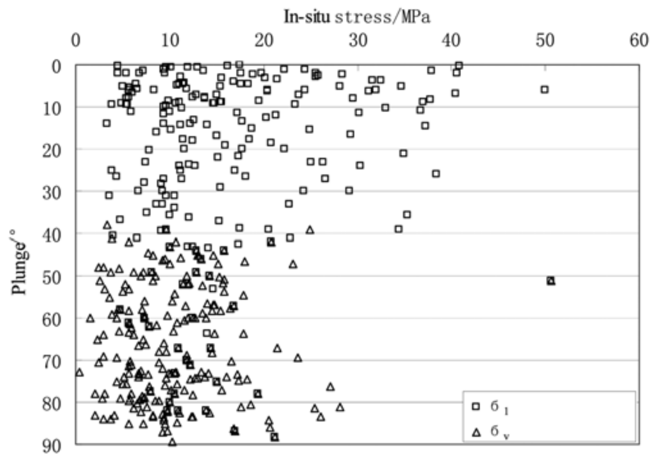

Fig. 8. Variation of in-situ stress plunges with data from OC and AE methods.

Dominantly, the σ_v is in plunges over 45°, while some of the σ_1 is also over 45°. This indicates that in those cases the σ_1 (dominant component of in-situ stress) is just the σ_v. The stereographic projection circles with rosette strikes of S_H drawn from HF, and pole plots of σ_1, σ_2 and σ_3 drawn from OC and AE techniques, are presented in Figure 9. Furthermore, the in-situ stress trends and plunges are presented in detail with values at 42 test sites in China (Fig. 9, Table 4), from HF with about 600 records, OC and AE with about 300 records. These sites were selected for the layout and design of tunnels or caverns for mining, transportation, or hydroelectric power stations, etc. The main difference between the plots in Figure 9 and the Chinese national stress map (Xie et al., 2007) is that all of the data in the former is from 847 in-situ stress records within depths of about 1,100 m. From Figure 9, it is known that the orientation of S_H is NEE in the northeast, NWW in the southeast, and NW and NE in the southwest of China.

3.3. Coefficients to Vertical Stress

The HF is commonly used for tunneling layout and design in China due to its obvious advantages as quick resolution and its principle easy to be understood (Table 1). The S_v is calculated as in Equation (1). Actually, in some coal mines in basins with a high thickness of Quaternary deposits incompletely consolidated, the γ is generally less than 0.027 MPa/m. This can be seen from Figure 10, where

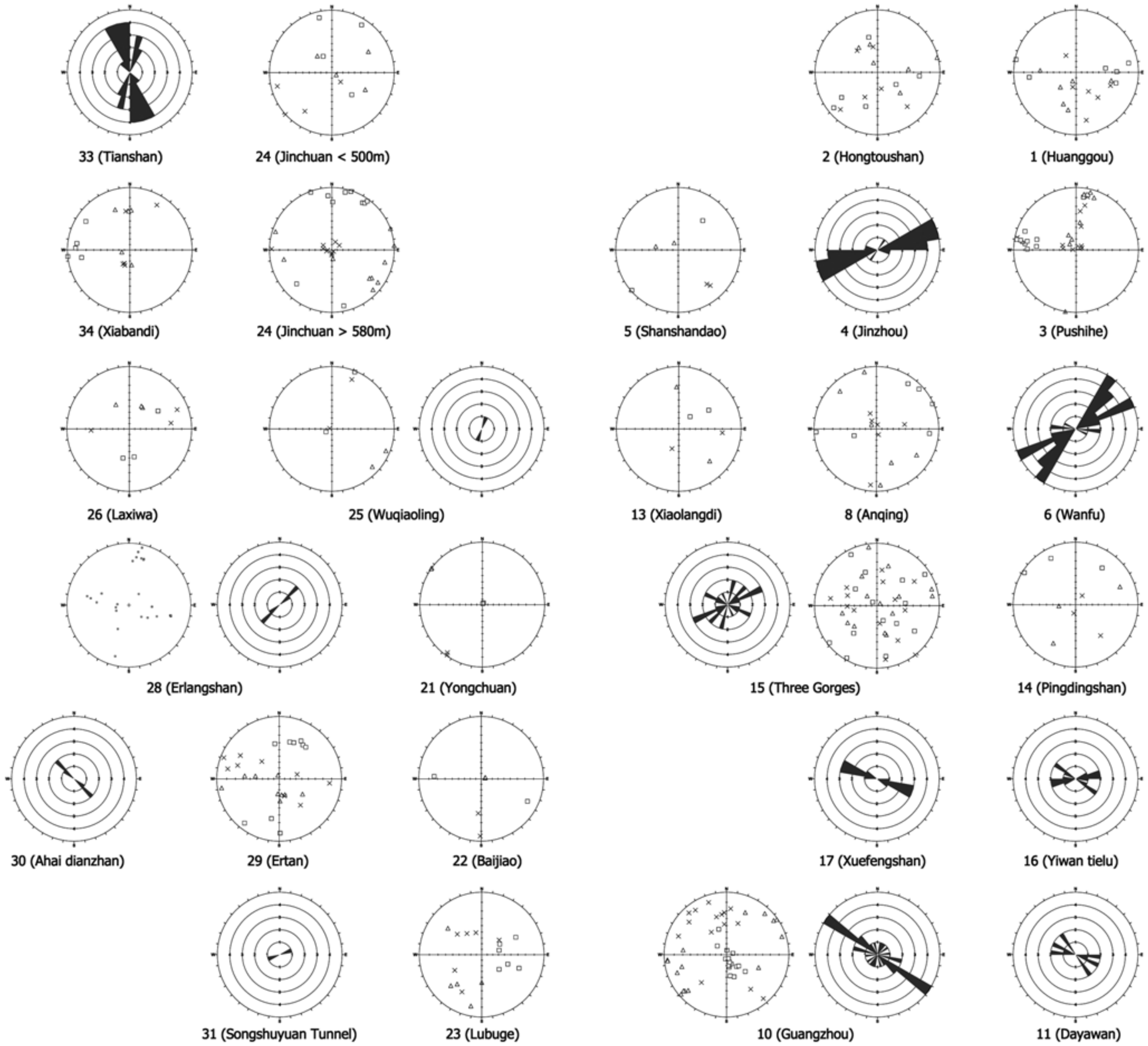

Fig. 9. Strikes and status in space of in-situ stress in China.

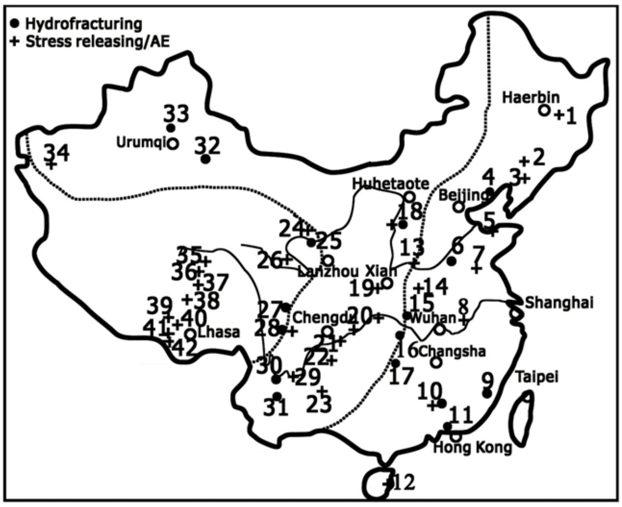

Fig. 9. (continued).

the S_v values are smaller in 37 records from the Wanfu Coal mine in eastern China, as No. 6 in Figure 9 and Table 4 (Cai et al., 2006). The relationships among the three components are just similar to those in Figures 4, 6 and 7. It also reveals the smaller magnitudes of S_v at depth of 800 to 1,100 m, together with greater differences in the three components at the same sites, although the differences will become smaller if the γ = 0.027 MP/m was used. The larger values of S_H, such as those in depths between 400 and 600 m, are examples from the Erlangshan Tunnel and the Tianshan Tunnel, No. 28–1 and 33, respectively, in southwest and west China. Figure 11 shows that the coefficient values of k and λ are generally less than 1.0 in depths larger than 600 m. For the same site and depth, the value of λ is larger than that of k, which indicates that in shallow depth, the S_H is more significant to analysis. Also the No. 6 case has a higher value (over 1.0) since its γ = 0.021 MP/m as the situation in Figure 10. Meanwhile, the largest values of coefficients belong to granites in very shallow depths in Jinzhou (No. 4) and Daya Bay (No. 11) (Fig. 11). The gently dipping joints at a shallow depth of less than 100 m are mostly attributed to these abnormal coefficient values. In granitic intrusion, residual stress is mostly in this kind of elastic rocks after they were exposed to ground under erosion and

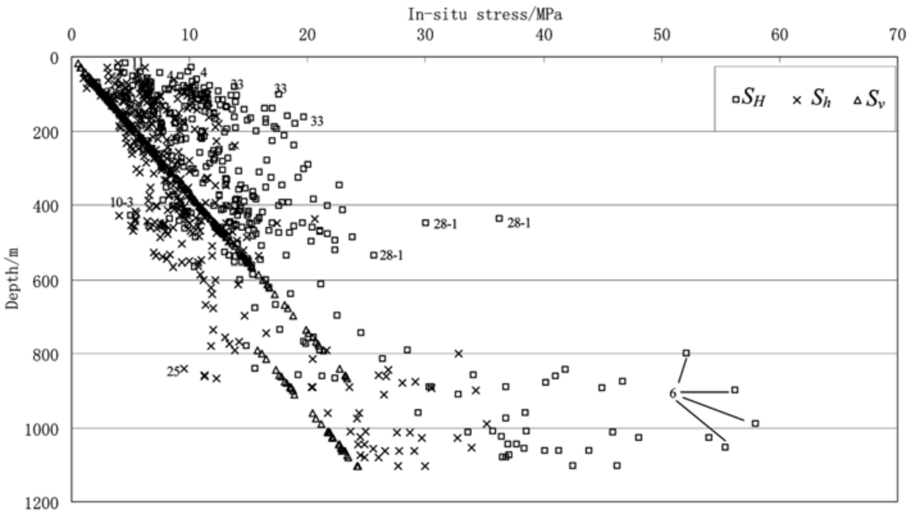

Fig. 10. Variation of three components of in-situ stress via HF technique with depth in China.

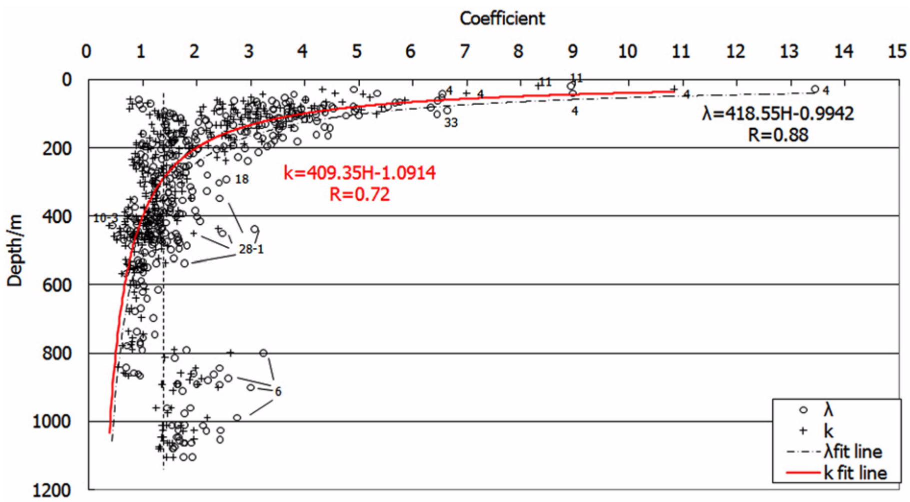

Fig. 11. Relationship between coefficients and depth for in-situ stress measurements in China.

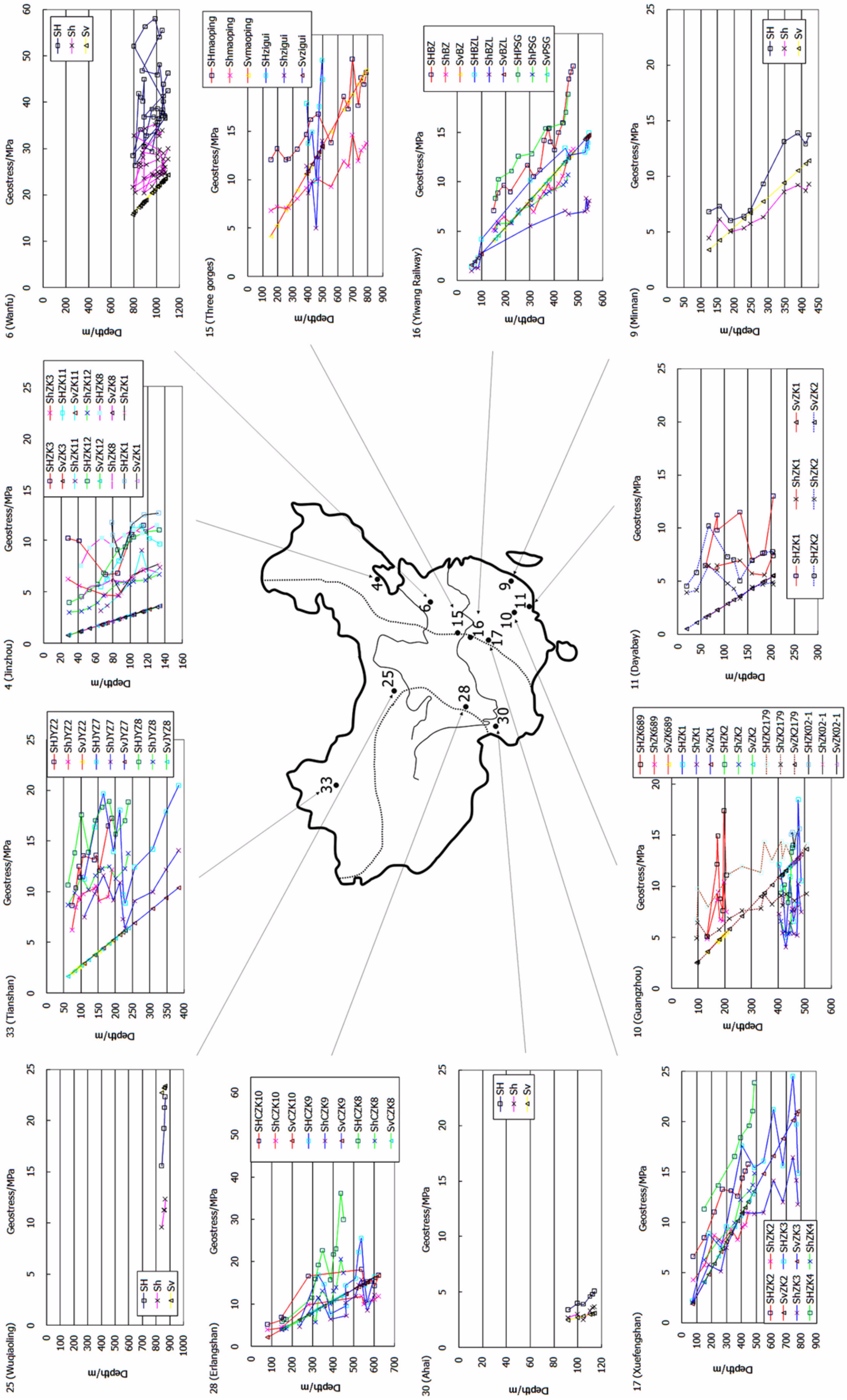

Fig. 12. Variation of in-situ stress with depth via HF technique in some sites of China.

unloading. For instance, it is inferred that the overlaying thickness over 900 m was erosed and unloaded resulting higher value of lateral coefficient λ in No. 11 (Shang et al., 2008). This situation seems to be true by just taking a look at Figure 4 for differentiation of the three kinds of lithology. The Sed behaves lower stress and lateral coefficient, but the Ig and Met, which often exposed to ground surface, behave larger stress and lateral coefficient values. For their S_H even near ground surface, the value is still very large.

These data can be used for a national comparison for their variations with depth. Figure 12 presents these variations with locations at three distinctive geomorphological settings. From east to west China, there are hills and plains, extensive plateau and basin, and the Qing-zang high plateau, at heights of <500 m, 1000~2000 m, >4000 m above sea level, respectively (Liu, 2007). From Figure 12, it can be seen that down to depths of 1,000 m, the S_H is commonly less than 25 MPa; only in the margins with high gradient topography is the stress as large as 40 MPa. To a depth of 300 m, the three component relations are varied to a great extent, mostly due to landform effects (secondary stress fields because of erosion and cutting as unloading functions). When depths are larger than 300 m, the stress values increase in a nearly constant gradient.

4. RELATED ENGINEERING GEOLOGICAL PROBLEMS

From Equation (7), it is inferred that for hard rocks with a saturated unaxial compression strength (σ_c) of 60 MPa, the boundary in-situ stress is at least 8.5 MPa and 15 MPa, respectively, to reach high and very high stress status. So from Figures 4 and 10, it is seen that with depths over 300 m, it is mostly potential high stress in soft and a few hard rocks. In depths over 600 m, the S_H is almost higher than 25 MPa; then if the σ_c is less than 100 MPa, the stress status is very high.

In China, some high in-situ stress values are associated with unfavorable engineering geological conditions. In western China with high in-situ stresses, unloading in banks of gorges and rock bursts in tunnels often occur. Among them, the most serious is the Ertan hydroelectric power station (No. 29) with core discs (Bai and Li, 1982). At a depth of 37.5 m, the S_H is 65 MPa (Fig. 4, Table 4). The qualitative evaluated major structural compression orientation is NNW, while the test result indicated that the S_H is in a trend of 20°. The angle between the two is 30~40°. Here, the Yalong River is in a strike of 300°. Such in-situ stress has been working perpendicular to the V-shape gorge strike. Just north of it, the Erlangshan Tunnel (No. 28) is famous for its rock burst taking account for 60% of the total length (Wang, 1998; Xu et al., 2003).

Another example is the Wuqiaoling tunnel (No. 25). The maximum buried depth is over 1,000 m, where the S_H at a depth of 866 m is 22.2 MPa in a trend of 22°. The tunnel axis is in an orientation of 343°, the included angle of the tunnel axis with the S_H is 39° (Guo et al., 2006). In excavation at weak rocks such as phyllite, slate and faulted rocks, large deformations such as squeezing occurred. The lateral walls convergence was 1,034 mm, and crown subsidence was 1,053 mm (Tao et al., 2005; An et al., 2007).

Deformation and failure patterns of crowns and side walls of tunnels are different. Therefore, in design and excavation, the shape and ratio of tunnel face, and reinforcement approaches are quite different. This can be seen from case studies in China. At site No. 29, the rock burst and flake usually occurred in adits with strikes of NW, just in a large inclined angle with the S_H (Bai and Li, 1982; Xue et al.,

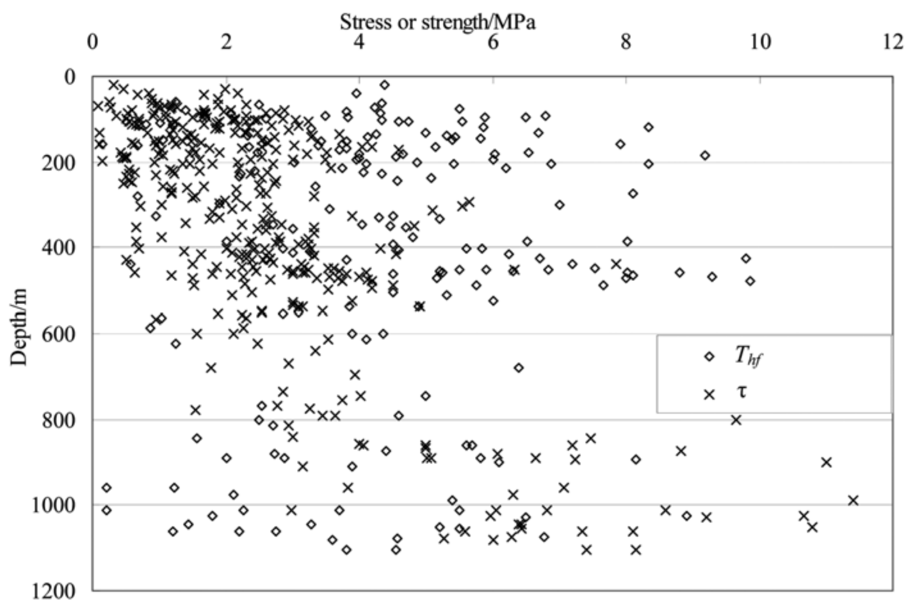

Fig. 13. The T_{hf} of rock mass and •Û from HF in China.

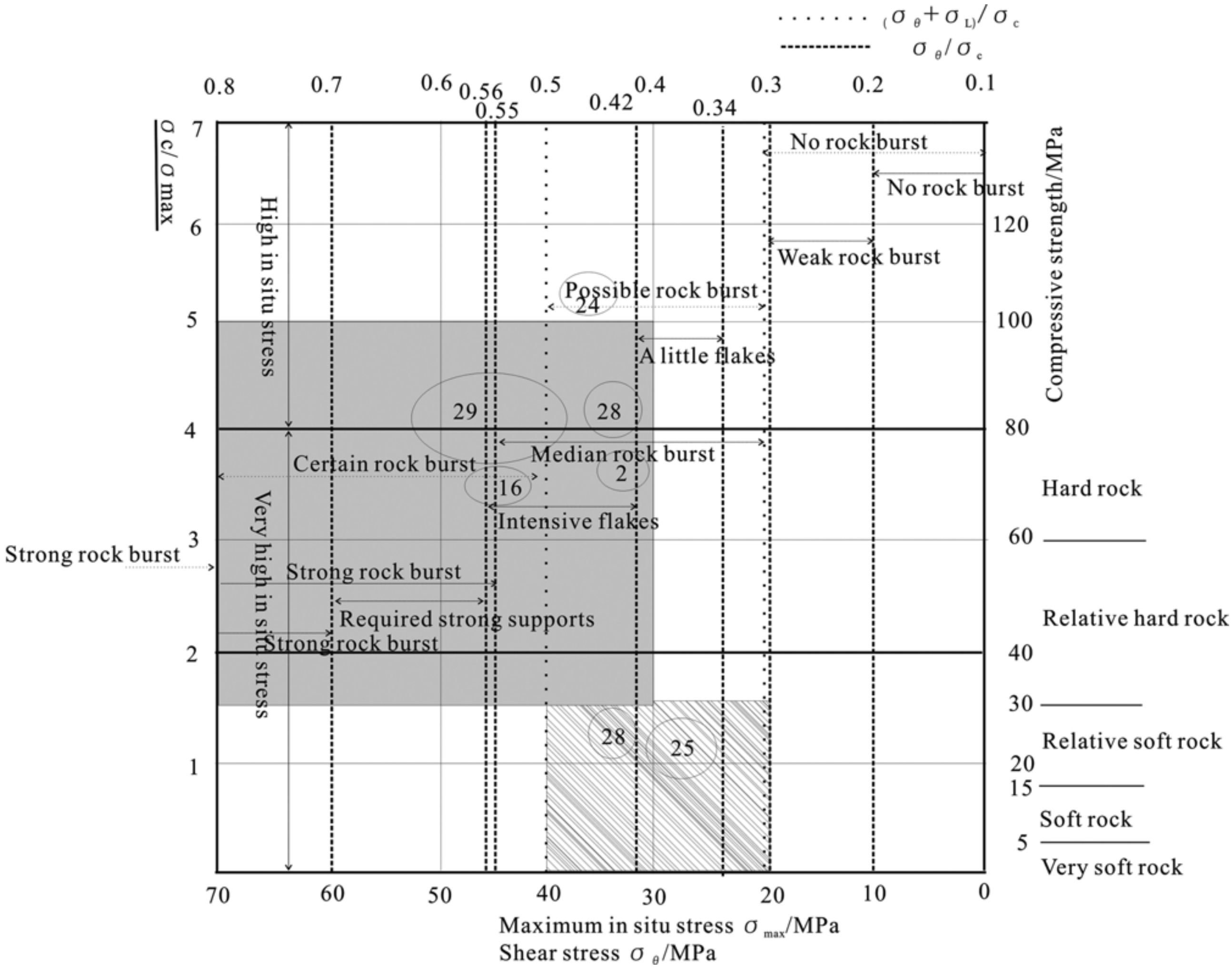

Fig. 14. Limit values for prediction of rock burst and squeezing from different aspect.

1987). In the Wuqiaoling Tunnel (No. 25), the tunnel shape was modified to a circle to pass through the hazards section with huge amounts of weak rocks, after a long time delay and budget had been spent to remedy large deformations and cave-in accidents because of very high stresses.

From HF tests, two indices can be calculated from recorded parameters as in Equations (5) and (6). Figure 13 shows the T_{hf} of rock mass and τ in boreholes in China. The former is densely plotted as 2~8 MPa, and the latter is widely spread from being very small to about 12 MPa within a depth of 1,200 m. So the values vary in this range, depending mostly on fractures of the measured sections, and the τ varies with a tendency to increase with depth.

Figure 14 shows limitary values for prediction of rock burst and squeezing from different relations of stress with strength. The gray frame represents the area of hard rocks with rock burst, while the oblique line frame represents the area of weak rocks with squeezing. The maximum in-situ stress (σ_{max}), compressive strength (σ_c), and ratios of tangential stress σ_θ with σ_c, and ratios of σ_θ and axial stress (σ_L) with σ_c are presented. The limitary values are combined according to rock burst predictions from different authors and institutes.

The IYRWR (1995) is on in-situ stress classification (σ_c/σ_{max}) and classification of σ_c. Russenes (1974) is on the ratio of σ_θ/σ_c for Norway rocks. Turchaninov et al. (1972) is on the ratio of $(\sigma_\theta+\sigma_L)/\sigma_c$ based on experiences in mining of Kolskiy Pov. Hoek and Brown (1997) is on that of σ_θ/σ_c at tunnels for mining in South Africa.

The numbers in circles are those 6 case examples with engineering geological problems as listed in Table 4. The area of circle is a very coarse estimation of the characteristics with respect to in-situ stress and intense of engineering geological problems as in Table 4.

5. CONCLUSIONS

From an overview of worldwide in-situ stress values, it is known that some extraordinary values over 50 MPa appear in hard rocks, such as igneous and metamorphic rocks, at depths no larger than 2,000 m. The S_H can be abnormally large in some cases, contributing to rock burst and squeezing in tunneling projects. At shallow depths, a little more horizontal stress is favorable for the stability of the crown. But in deep tunnels, the effect is very different, usually causing engineering geological problems. The most typical examples in China are the Ertan, Erlangshan, and Wuqiaoling tunnels, numbered 29, 28 and 25, respectively. Located at the margins of Qing-zang Plateau, they are mostly at shallow depths at the banks of large gorges or in depths larger than 300 m.

The coefficient λ of igneous and metamorphic rocks is generally larger than that of sedimentary rocks because of their formation in large depth and residual horizontal stress due to erosion and unloading in ground surface.

As for the relationship between σ_v and S_v, the depth limits of 300 m and 1,000 m must be paid more attention. In large depths over 1,000 m, the difference of the two is very obvious. Then the unit weight value of 0.027 MPa/m in rock or as little as 0.021 MPa/m in some Quarternary sedimentary basins can affect the ratio of k and λ values to a large extent.

ACKNOWLEDGMENTS: The authors appreciate supports from the Special Funds for Major State Basic Research Project underGrant No. 2010CB732001, and the Brain Korea 21 Project in 2008 and the Research Institute of Engineering Science, Seoul National University.

REFERENCES

An, R., Liu, W., and Liu, Z., 2007, Deformation characteristics analysis of extrusion rock tunnel. Journal of Shijiazhuang Railway Institute, 20, 14–18 (in Chinese with English abstract).

Bai, S. and Li, G., 1982, Research on Stress Field around Dam Area of Ertan Hydropower Station. Chinese Journal of Rock Mechanics and Engineering, 1, 45–55 (in Chinese).

Boyce, G.M., 1981, A study of the acoustic emission response of various rock types. M.Sc. Thesis, Drexel University, Philadephia, 170 p.

Bieniawski, Z.T., 1984, Rock Mechanics Design in Mining and Tunneling. Balkema, Rotterdam, 209 p.

Brown, E.T. and Hoek, E., 1978, Trends in relationships between measured in–situ stresses and depth. International Journal of Rock Mechanics and Mining Science & Geomechanics Abstracts, 15, 211–215.

Cai, M., Qiao, L., Yu, B., and Wang, S., 1999, Results and analysis of in–situ stress measurement at deep position of No. 2 mining area of Jinchuan Nichkel mine. Chinese Journal of Rock Mechanics and Engineering, 18, 414–418 (in Chinese with English abstract).

Cai M., Qiao L., Li C., Yu B., and Wang S., 2000, Results of in situ stress measurements and their application to mining design at five Chinese metal mines. International Journal of Rock Mechanics and Mining Sciences, 37, 509–515.

Cai M., Yu B., Qiao L., Chen G., and Li C. 1997, Experience of in situ stress measurement with hydrofracturing and overcoring techniques in Ekou Mine, China. International Journal of Rock Mechanics and Mining Sciences, 34, 299–302.

Cai, M., Chen, C., Peng, H., Ji, H., Qiao, L., and Tan, Z., 2006, In–situ stress measurement by hydraulic fracturing technique in deep position of Wangfu coal mine. Chinese Journal of Rock Mechanics and Engineering, 25, 1069–1074 (in Chinese with English abstract).

Chen, J., Cao, X., and Li, Z., 1982, Hydraulic fracturing technique applied to test deep in–situ stress in North China. Seismic Journal, 4, 350–361.

Chen, Q., Zhu, B., and Hu, H., 2006, Experimental research on measurement of in–situ stress field by Kaiser Effect. Chinese Journal of Rock Mechanics and Engineering, 25, 1370–1376 (in Chinese with English abstract).

Choi, S.O., 2007, A decade's hydrofracturing experiences of in–situ stress measurement for tunnel construction in Korea. Chinese Journal of Rock Mechanics and Engineering, 26, 2200–2206.

Dong, C., Wang, L., Yang, X., Wang, H., and Wang, W., 2001, Stress measurement of Anqing Copper Mining. Journal of Geomechanics, 7, 259–264 (in Chinese with English abstract).

Engelder, T., 1993, Stress regimes in the lithosphere. Princeton University Press, Princeton, 475 p.

Fairhurst, C., 2003, Stress estimation in rock: a brief history and review. International Journal of Rock Mechanics and Mining Sciences, 40, 957–973.

Feng, Y., 1996, In–situ stress measurement via acoustic emission at underground powerhouse of Xiaolangdi Hydraulic network. Journal of Yangtze River Scientific Research Institute, 13(Supp.), 62–65 (in Chinese).

Gay, N.C., 1975, In–situ stresses measurements in sourthern Africa. Pure and Applied Geophysics, 115, 3–10.

Gou, P. and Zhang, Y., 2002, Measurement of earth stress and its analysis in the 1st coal mine of Pingdingshan Coal Industrial (Group) Company. Journal of Jiaozuo Institute of Technology (Natural Science), 21, 15–19 (in Chinese with English abstract).

Guo, Q., An, Q., and Zhao, S., 2002, Application of hydraulic fracturing test in the design of Guangzhou Pump Storage Project. Chinese Journal of Rock Mechanics and Engineering, 21, 828–832 (in Chinese).

Guo, Q., Wu, F., Qian, W., and Zhang, Y., 2006, Study on relationship between deformation of surrounding rock and in–situ stess in Wushaoling deep-buried railway tunnel. Chinese Journal of Rock Mechanics and Engineering, 25, 2194–2199 (in Chinese).

Hast, N., 1958, The measurement of rock pressure in mines, Årsbok. Sveriges Geologiska Undersökning, Series C, 52, 1–183.

Hast, N., 1973, Determination of the state of stresses in the upper part of the Earth's curst. Tectonophysics, 12, 169–211.

Haimson, B.C. and Cornet, F.H., 2003, ISRM Suggested Methods for rock stress estimation – Part 3; hydraulic fracturing (HF) and/or hydraulic testing of pre-existing fractures (HTPF). International Journal of Rock Mechanics and Mining Sciences, 40, 1011–1020.

Heidbach, O., Tingay, M., Barth, A., Reinecker, J., Kurfeß, D., and Müller, B., 2008, The World Stress Map database release 2008. doi:10.1594/GFZ.WSM.Rel2008, (available online at www.world-stress-map.org).

Hoek, E. and Brown, E.T., 1997, Practical estimates of rock mass strength. International Journal of Rock Mechanics and Mining Sciences, 34, 1165–1186.

Hou, Y., Sun, W., Chen, Q., and Wang, B., 2006, Chen S. In–situ stress measurement and its application in the pre-feasibility study of an underground oil reservoir in China. Journal of Geomechanics, 12, 197–202 (in Chinese).

Imrie, A.S. and Jory, L.T., 1968, Behavior of the underground powerhouse arch at the W.A.C. Bennett dam during excavation. In:

Proceedings of the 5th Canadian Rock Mechanics Symposium, Toronto, Canada, 19–39.

IYRWR (Institute of Yangtze River Scientific Research, Ministry of Water Resources), 1995, Standard for engineering classification of rock masses (GB5021894). China Planning Press, Beijing, 78 p. (in Chinese).

Jin, X.G., Li, X.H., Wang, L.S., and Li, Y.L., 2001, Deformation characters and application practice of different surrounding rocks class of highway tunnel in high in–situ stress area. Chinese Journal of Rock Mechanics and Engineering 20 (suppl.), 932–935 (in Chinese with English abstract).

Kang, Y., Li, X., Wang, Q., and Jiang, Y., 2005, Research on in–situ stress measurement and rockburst forcast in tunnels. Rock and Soil Mechanics, 26, 959–963 (in Chinese).

Leeman, E.R., 1964, The measurement of stress in rock. Journal of the South African Institute of Mining and Metallurgy, 65, 45–114.

Li, F., Zhang, B., and Su, K., 1993, Reservior-induced earthquake in dam site — in–situ stress measurement and analysis in boreholes of Maoping. Seismic Press House, Beijing, 220 p. (in Chinese).

Li, J., Peng, H., Gui, W., Ma, X., Yang, S., and Liao, J., 2005, Results of rock stress measurements and engineering application of a railway tunnel in Northwestern Yunnan. Journal of Geomechanics, 11, 135–144 (in Chinese).

Liang, G. and Pan, Y., 1989, Back analysis of in–situ stress at level 635 at Longfeng Mine of Fushun, China. Chinese Journal of Rock Mechanics and Engineering, 8, 330–336 (in Chinese with English abstract).

Liao, C. and Shi, Z., 1983, In–situ stress measurements and their application to engineering design in the Jinchuan Mine. Chinese Journal of Rock Mechanics and Engineering, 2, 103–112 (in Chinese).

Linder, E.N. and Haipern, J.A., 1978, In–situ stress in north America: a compilation. International Journal of Rock Mechanics and Mining Sciences, 15, 1–14.

Liu, M.G., 2007, Alta of Chinese natural geography. China Map Press, Beijing, 252 p. (in Chinese).

Liu, Y., Gong, B., Xiao, B., and Luo, C., 1990, Analyses of ground stress field in underground excavation of Guangzhou Pumped Storage Power Station. Journal of Yangtze River Scientific Research Institute, 4, 45–53 (in Chinese).

Liu, Y., Gong, B., Zhong, Z., and Xiao, B., 1992, A preliminary exploration of in–situ stress field for the Lock Area of the Three Gorges Project. Journal of Yangtze River Scientific Research Institute, 29, 77–98 (in Chinese).

Liu, Y., Yin, J., and Liu, Y., 2004, Measurement and study of in–situ stresses for the Xiabandi Hydraulic Project, Xinjiang. Chinese Journal of Rock Mechanics and Engineering, 23, 242–246 (in Chinese).

Liu, Y. and Xiao, B., 2005, Study on seismic activity and in–situ stress in west China. Chinese Journal of Rock Mechanics and Engineering, 24, 4502–4508 (in Chinese).

Ma, X., Peng, H., and Li, J., 2005, Application of hydraulic fracturing in–situ stress measurements in tunneling in western Xinjiang. Journal of Geomechanics, 11, 386–393 (in Chinese).

Peng, H., Cui, W., Ma, X., and Li, J., 2006, Hydraulic fracturing in–situ stress measurements of the Water Diversion area in the first stage of the SouthNorth Water Diversion Project (Western Line). Journal of Geomechanics, 12, 182–190 (in Chinese).

Pine, R.J., Tunbrdge, L.W., and Merrififld, C.M., 1983, In–situ stress measurement in Carnmenells Granite: overcording tests at south Croftg mines at a depth of 790m. International Journal of Rock Mechanics and Mining Sciences, 20, 54–72.

Qiao, X., Liu, C., Xu, B., and Zhou, F., 2001, In–situ stress study of Baka oilfield and its application. Xinjiang Geology, 19, 300–304 (in Chinese).

Russenes, B.F., 1974, Analysis of rock spalling for tunnels in steep valley sides (in Norwegian). M.Sc. thesis, Norwegian Institute of Technology, Department of Geology, 247 p.

Rutqvist, J. and Stephansson, O., 1996, A cyclic hydraulic jacking test to determine the in–situ stress normal to a fracture. International Journal of Rock Mechanics and Mining Science & Geomechanics Abstracts, 33, 695–711.

Shang, Y.J., Park, H.D., Yuan, G.X., Sun, Y.C., and Gao, Q., 2008, From in situ stress and discontinuities to the strength of granites: comparison and case study. Geosciences Journal, 12, 361–372.

Sjoberg, J., Christiansson, R., and Hudson, J.A., 2003, ISRM Suggested Methods for rock stress estimation – Part 2: overcoring methods. International Journal of Rock Mechanics and Mining Sciences, 40, 999–1010.

Su, H., Huang, J., and Li, X., 1994, Research on rock stress field around mining area of BaiJiao. Journal of Southwest Institute of Technology, 9, 59–64 (in Chinese with English abstract).

Sun, G., 1993, Engineering geology and geoengineering, Seismic Press House, Beijing, 218 p. (in Chinese).

Sun, S., Guo, J., Ding, J., Guo, Q., and Liang, G., 1991, Hydraulic fracturing in–situ stress measurement at the Guangzhou Pumped Storage Power Plant. Chinese Journal of Rock Mechanics and Engineering, 10, 374–381 (in Chinese with English abstract).

Tan, C., Sun, W., Sun, Y., and Wang, L., 2006, A consideration on in–situ crustal stress measuring and its underground engineering application. Acta Geologica Sinica, 80, 1627–1632 (in Chinese).

Tao, B., Wu, F., Guo, Q., and Guo, G., 2005, Research on rheology rule of deep-buried long tunnel of Wuqiaoling under high crust stress. Earth and Environment, 33(Suppl.), 304–308 (in Chinese).

Turchaninov, I.A., Markov, G.A., Gzovsky, M.V., Kazikayev, D.M., Frenze, U.K., Batugin, S.A., and Chabdarova, U.I., 1972, State of stress in the upper part of the Earth's crust based on direct measurements in mines and on tectonophysical and seismological studies. Physics of the Earth and Planetary Interiors, 6, 229–234.

Wang, L., Ding, Y., Liu, Q., Shao, Z., Tan, C., Wang, W., and Chen, G., 1996, Rock stress measurements in a planned tunnel for diversion of water from the Yellow River. Journal of Geomechanics, 2, 62–69 (in Chinese with English abstract).

Wang, S.J., Yang, Z.F., and Liu, Z.H., 1984, Stability analysis of rock mass for underground engineering projects, Science Press, Beijing, 282 p. (in Chinese).

Wang, C., 1998, The measure of ground stress in road tunnel axis of Erlang Mountain. Coal Geology and Exploration, 26 (Suppl.), 43–45 (in Chinese).

Wei, F., Hu, G., Wang, H., Yuan, Z., and Fan, X., 2007, Measurement and characteristics of in–situ stress variation at Yongchuan Coal Mine. Mining Safe and Envrionment Preservation, 34, 1–6 (in Chinese).

Wototniki, G. and Denham, D., 1976, The state of stress in the upper part of the Earth's crust in Australia according to measurements in tunnels and mines and from seismic observations. In: Proceedings of the 8th Symposium of International Society on Rock Mechanicson on Investigation of stress in rock-advances in stress measurement. Sydney, Australia, 71–82.

Wu, M., Zhang, C., Liao, C., Ma, Y., and Ou, M., 2005, The recent state of stress in the central Qinghai-Tibet Plateau according to in–situ stress measurements. Chinese Journal of Geophysics, 48, 327–332 (in Chinese).

Wu, M. and Liao, C., 2000, Stress measurements and study of stability of the Damao Tunnel. Journal of Geomechanics, 6, 71–76.

Wu, M., Zhang, C., Liao, C., and Ou, M., 2004, Stress measurement and engineering stability analysis at Fenghuoshan Tunnel. Acta Geoscientia Sinica, 26, 71–74 (in Chinese).

Wu, M., Li, G., Liao, C., and Dong, C., 2006, Measurements of in–situ stress in the Pushihe Hydropower Station, Liaoning. Journal of Geomechanics, 12, 191–196 (in Chinese).

Wu, M., Liao, C., and Yuan, J., 2002, A study of stress state and engineering stability of underground houses at the Huanggou Accumulation Power Station. Acta Geoscientia Sinica, 23, 263–268 (in Chinese).

Xiao, B., Luo, C., and Liu, Y., 2005, In–situ stress measurement and prediction analysis of tunnel rockburst in west Hubei. Chinese Journal of Rock Mechanics and Engineering, 24, 4472–4477 (in Chinese with English abstract).

Xiao, B.Z., 2007, Study on characteristics of geological stress field in the line engineering. Blasting, 24(Album), 234–239 (in Chinese with English abstract).

Xie, F.R., Chen, Q.C., and Li,H., 2007, Fundamental database of crustal stress environment in continental China. Progress in Geophysics, 22, 131–136 (in Chinese with English abstract).

Xu, L., Wang, L., Sun, Z., and Xu, J., 2003, In–situ stress measurement in rockmass of Erlang Mountain Highway Tunnel. Chinese Journal of Rock Mechanics and Engineering, 22, 611–614 (in Chinese with English abstract).

Xue, X., Guo, H., and Ma, Q., 1987, High in–situ stress in rock mass and analysis. Journal of Hydraulic Engineering, 3, 52–58.

Yang, Z.F., Wang, Z.Y., Zhang, L.Q., Zhou, R., and Xing, N.X., 2001, Back-analysis of viscoelastic displacements in a soft rock road tunnel. International Journal of Rock Mechanics and Mining Sciences, 38, 331–341.

Yao, B., Liu, Z., and Wang, J., 1995, Research on characteristics of field stress in Sanshandao gold mine area. Journal of Engineering Geology, 3, 21–28 (in Chinese).

Yin, J., Chen, L., and Zhong, Z., 2001, Measurement and interpretation on in–situ stresses with hydro-fracturing in a highway tunnel site. Chinese Journal of Rock Mechanics and Engineering, 20(Supp.), 1827–1830 (in Chinese with English abstract).

Yu, X.F., Zheng, Y.R., and Liu, H.H., 1983, Stability analysis of surrounding rock in underground engineering. China Coal Industry Press, Beijing, 619 p. (in Chinese).

Yuan, D., Mei, Y., and Qin, X., 1996, Crustal stability analysis on dam site and nearby area of Three Gorges Project. China University of Geosciences, Wuhan, 11–17 (in Chinese).

Zhang, C., Wu, M., Liao, C., Ma, Y., and Ou, M., 2007, The result of current stress measurements and stress state in the region of YangbajainKangmar in Tibet. Chinese Journal of Geophysics, 50, 517–522 (in Chinese).

Zhang, Z., Wang, L., and Li, T., 2005, Study on the in–situ stress field in the Xuefeng Mountain expressway tunnel. The Chinese Journal of Geological Hazard and Control, 16, 86–89 (in Chinese).

Zhao J., Hefny A.M., and Zhou Y.X., 2005, Hydrofracturing in situ stress measurements in Singapore granite. International Journal of Rock Mechanics and Mining Sciences, 42, 577–583.

Zhou, C., Ai, K., Yin, J., and Liu, Y., 2006, Experimental study on geostress field and rock mass mechanical characters in dam site slope of Buxi Hydropower Station. Chinese Journal of Rock Mechanics and Engineering, 25 (Supp. 2), 3959–3964 (in Chinese with English abstract).

Zhou, C., Yin, J., Liu, Y., and Guo, X., 2007, In–situ stress measurement and evaluation for Ahai Hydro-power station's dam site. Journal of Yangtze River Scientific Research Institute, 24, 68–71 (in Chinese).

Zhou, G., Li, Y., and Wu, Z., 2005, Measurement of crustal stress and analysis of characteristics in Datun mining area. Journal of China Coal Society, 30, 314–318 (in Chinese with English abstract).

Zhu, H. and Tao, Z., 1994, In–situ stress distribution in different rocks. Acta Seismologica Sinica, 16, 49–63 (in Chinese).

Manuscript received August 5, 2009
Manuscript accepted March 24, 2010